CHAPTER 1

Introduction

What emptiness do you gaze upon! – Rabindranath Tagore

The gamut of astronomical sources consists of the relatively near-earth solar system objects to the far-flung galaxies and the active galactic nuclei such as quasi-stellar radio objects or quasars. Planets in the solar system, stars in a galaxy, the interstellar medium, galaxies and clusters of galaxies are the building blocks that constitute the physical Universe. These astronomical sources represent various physical sizes, distances (from the earth) and other physical parameters such as temperature, density, fields, and timescales characterising the physical processes that account for their behaviour. In a way one may categorize the objects into two groups namely, the point sources such as stars that generally cannot be resolved by a telescope, and extended sources such as gaseous and diffuse nebulae in our Galaxy and nearby external galaxies. This categorization necessarily depends on the distance as well. Let us loosely categorize that any object of angular size less than a second of arc may be considered as a point source and any object that has an angular size more than a second of arc as an extended source. With that being said, we hasten to add here that using modern technological advances, sub-arcsecond observations have become possible with telescopes of large diameters. This categorization reflects basically the observer's inability to resolve a celestial object beyond a certain degree of spatial dimension. We shall elaborate this aspect in Chapter 2. Celestial objects in general reveal themselves by the emission of electromagnetic radiation. While it is conceivable that an object emits radiation, in principle, in the entire electromagnetic spectrum (like for instance a black body), the possibility of detection of the radiation depends on the wavelength range in which the emission occurs predominantly, as decided by various physical conditions of the source. This aspect will be elaborated in Chapter 3. As shown in Table 1.1, the wavelength (λ) or frequency (ν) of the radiation and hence its associated energy varies from milli-electron volts in the radio regime to higher than mega-electron volts in the most energetic radiation towards the gamma-ray end of the spectrum. The table also lists out observable features that include continuum and/or discrete radiation processes (see Chapter 3 for details). Clearly, therefore, the observational techniques involving telescopes and detectors would be

quite different for different wavelength regimes. Accordingly, based on the wavelength regime and hence on the observational and detection technique, astronomical observations may be divided into various sub-branches, namely, Optical (visible), Infrared (IR), Ultra-Violet (UV), Radio, X-ray, and gamma-ray astronomies. Further, the presence of the earth's atmosphere intervening the line of sight between the observer and the celestial object, the celestial radiation gets impeded due to absorption and scattering by the constituents of the atmosphere. Fig 1.1 depicts the atmospheric effect on the radiation for the entire electromagnetic spectrum as it penetrates through the atmosphere. While the visible and radio regimes get through unhindered, other wavelength ranges such as ultraviolet, infrared, and sub-millimetre radiation undergo severe extinction (a term that accounts for both scattering and absorption). The main absorbers are water vapour, carbon dioxide and ozone in the lower atmosphere for infrared region, nitrogen and oxygen gases in the upper atmosphere and ozone in the stratosphere for energetic radiation. Radio waves of long wavelengths (greater than about 30 m or low frequencies less than about 10 MHz) are reflected out by the plasma of the Earth's topside (above the height of maximum plasma density) of Ionosphere. At frequencies below 1 MHz the interplanetary and interstellar plasma makes it impossible for observations (Longair 2011).

Table 1.1: Electromagnetic Radiation and observable features.

EM Radiation	E(eV)	λ	ν(Hz)	Observables Features
Gamma Rays	1-1000x10^{6}	$< 10^{-11}$ m	2x10^{20}-2x10^{23}	Nuclear
Hard X-rays	2-10x10^{3}	0.025–0.25 nm	4x10^{17}-2x10^{20}	Thermal Bremsstrahlung
Soft X-rays	0.1-2x10^{3}	0.25-10 nm	3x10^{16}-4x10^{17}	Atomic Inner Shell
EUV	13.6-100	10 – 91.2 nm	3x10^{15}-3x10^{16}	Atomic / Continuum
UV	4-13.6	91.2 - 300 nm	1x10^{15}-3x10^{15}	Atomic / Molecular
Optical	1.25-2.5	400 - 800 nm	4x10^{14}-7x10^{14}	Atomic / Molecular
Near-IR	0.17-1.25	0.8 - 6 μm	4x10^{14}-7x10^{14}	Vibrational
Mid-IR	0.03 -0.17	6 - 35 μm	1x10^{13}-5x10^{13}	Rotational / Dust
Far-IR	3x10^{-3} -0.03	35 - 300 μm	1x10^{12}-1x10^{13}	Rotational / Dust
Sub-mm	1x10^{-3}-3x10^{-3}	300 - 1000 μm	3x10^{11}-1x10^{12}	Rotational
Radio/mm	1x10^{-7}-1x10^{-3}	0.1 cm – 10 m	3x10^{7}-3x10^{11}	Non-thermal

To observe the radiation in the "block out" frequency regimes it is necessary to circumvent the atmospheric effect by flying instruments onboard balloons, aircrafts and spacecrafts as the situation demands (see Fig 1.1). Based on this we can also divide the astronomical observations into two broad classes – ground-based (for optical, near-infrared and radio wavelengths) and space-based astronomies (for UV, far-infrared, X-rays). Very high energy radiation detection is made from ground-based secondary radiation detection.

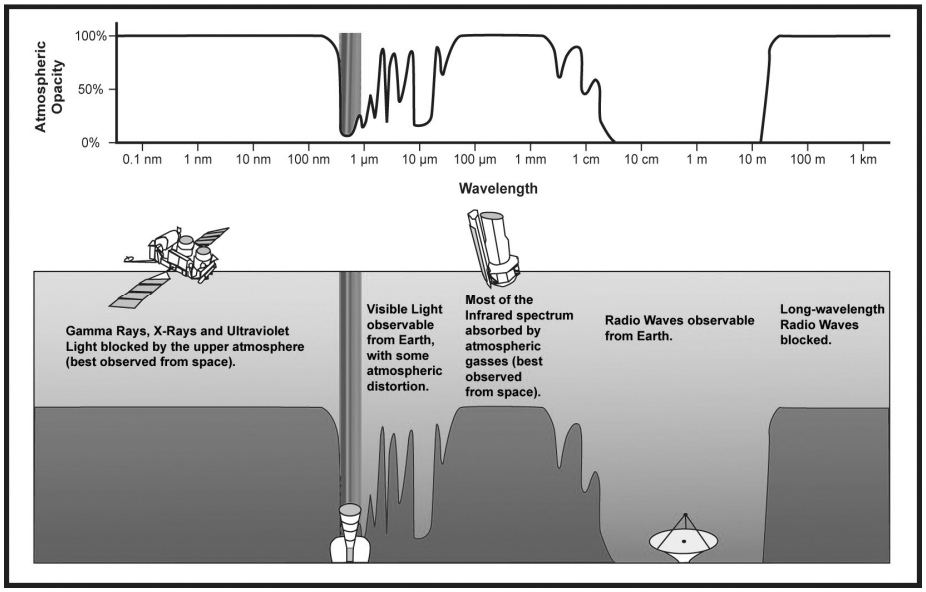

Figure 1.1: Atmospheric opacity for electromagnetic spectrum from high energy gamma rays (at left) to low energy radio waves (to the right). The top panel shows the atmospheric opacity as a function of wavelength. The bottom panel shows the observational means at different wavelength regimes. The narrow vertical dark band shows the visible wavelength range that gets through to the ground level along with some bands in near-infrared. Radio waves get through unhindered (from NASA website).

1.1 Definition of Important Terminology used in Astronomy

Astronomers use certain scientific terminology specific to celestial observations to quantify the measured radiation and other physical parameters. We define such terminology in the following sub-sections.

1.1.1 Intensity and Specific Intensity: Intensity is source specific – measured at the source of radiation. Intensity is the power emitted by unit area of a source into a unit solid angle. It is designated as I and is given in

Watts/steradian/m^2. Specific intensity I_λ is intensity measured in each narrow interval of spectral wavelength and is given in Watts/steradian/m^2/μm. In the units for specific intensity, /μm is usually used for infrared radiation; and /nm or /Å may be used of visible light.

1.1.2 Luminosity: Luminosity, like Intensity, is also source specific. It is the total flow of radiation emanating from a source of effective temperature T and radius R. It is measured in Watts (Joules/s). It is given by,

$$L = 4\pi R^2 \sigma T^4 \tag{1.1}$$

where σ is Stefan-Boltzmann constant. The luminosity in each narrow spectral bandwidth is called monochromatic luminosity (L_λ) given in W/μm.

1.1.3 Flux Density: While intensity and luminosity are defined specifically to characterise a source, flux density is what the observer measures on a detector. It is the power received from a source in unit frequency or wavelength measured in W/m^2/Hz or W/m^2/μm respectively. Following the inverse-square-law of light intensity for a point source, the flux is given by luminosity divided by the surface area of an imaginary spherical shell whose radius d is equal to the distance of the source to the observer: $F = L / (4\pi d^2)$. Thus, luminosity is a measure of radiant energy at the source while flux is the same but measured at the observer.

1.1.4 Parsec and Light-year: Astronomers use distance scales that are very specific. For example, the astronomical unit (AU) is the average distance ~ 1.49 x 10^{11} m between the Earth and the Sun. This unit is specifically used for the sizes of the debris around a star, or the distances of planets from their parent star. The most familiar term, known as the light-year, is the distance travelled by a photon in one year and is given by 9.46 x 10^{15} m. The unit of distance that is more popular among astronomers is parsec (short for "parallax second"), for distances larger than the size of the solar system. Parallax (see Fig. 1.2 for definition) is a measure of distance based on the apparent shift of the position of a celestial object as observed from the Earth at two diametrically opposite positions in Earth's orbit around the Sun. Parsec is defined as the distance at which the radius of the Earth's orbit around the Sun (= 1 AU) subtends an angle of parallax of one arcsecond. It is equal to 3.08 x 10^{16} m. A parsec is thus ~ 3.25 times the light year. In general, if the angle of parallax for a star is p arcsec, then its distance is $d = p''$parsec or pc (see Fig. 1.2).

1.1.5 The Magnitude System: Traditionally astronomers (since Hipparchus in the 2nd century BCE) use a brightness unit, known as the magnitude system, to quantify the brightness of a star. Magnitude denoted as 'm' is a

relative logarithmic scale giving the brightness of a star with respect to that of a standard star whose brightness or magnitude, m_0 is already known.

$$m - m_0 = 2.512\ log_{10}\left(\frac{F_0}{F}\right)$$

or

$$F = F_0 10^{-0.4(m-m_0)} \tag{1.2}$$

with F and F_0 being the fluxes (Watts/m^2/Hz). According to this definition, a star of higher magnitude is fainter than a star of lower magnitude. A magnitude difference of 5 between two stars indicates 100 times in their brightness ratio ($2.512^5 = 100$). It is normal practice to consider a main sequence (dwarf) star of spectral type A0 (having effective temperature of about 10000 K; in comparison the Sun is also a dwarf star but of G3 spectral type having an effective temperature of 5875 K) for a standard star wherein its magnitude in all the spectral bands as considered as 0. The star α Vega of spectral type A0V fits the bill for flux-calibrating the optical and infrared observations (see Appendix A3 for Vega standard fluxes).

Using the above equation for flux and Vega as standard star having magnitude zero, we can also compute the number of photons emanating from a star of a given magnitude within a wavelength band, impinging upon a telescope,

$$n_p = \frac{3.64 \times 10^{-9}}{10^{0.4167m}}\ \Delta\lambda\ \frac{\pi D^2}{4}\ \frac{1}{h\nu}\ \frac{\pi\theta^2}{4} \tag{1.3}$$

with D the aperture or diameter of the telescope primary mirror (in cm), $\Delta\lambda$ bandwidth of incoming radiation of central wavelength λ (in Å units), θ the angular size of the star image formed on the detector and ($h\nu$) the photon energy at 0.55 μm and the numerical factor denotes the total energy flux (in ergs/s/cm^2/Å) from a standard star of 0th magnitude at 0.55 μm.

1.1.6 Apparent and Absolute Magnitudes and the Distance Modulus: The magnitude that we determine using the equation (1.2) gives apparent magnitude of a star relative to a standard star that has magnitude 0 at all wavelength bands. The apparent magnitude is related to the flux (luminosity divided by the square of the distance to the object) – the larger the distance the larger would be the magnitude for the same luminosity. It depicts the inverse square law for luminosity variation with distance to the source. So, the farther a star of a particular luminosity is situated the fainter it appears and hence the bigger would be its apparent magnitude (the bigger the magnitude the dimmer the object appears).

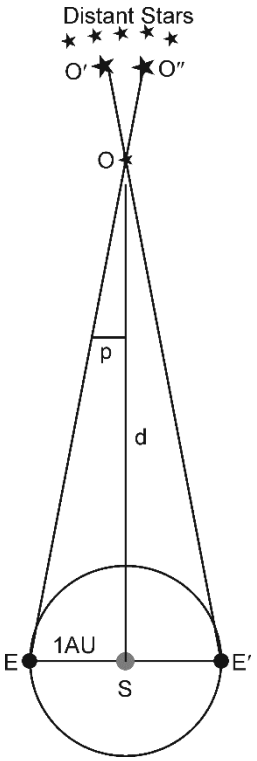

Figure 1.2: Definition of parallax. S and E denote the sun and the earth and the circle the orbit of the earth. A star O, at a distance *d*, will have an apparent shift in its position (denoted by O' and O" with respect to relatively distant stars when observed from two diametrically opposite positions E and E' in Earth's orbit around the Sun. The half-angle p (being very small) is called the parallax. The distance at which a parallax of 1 arcsec occurs is defined as 1 parsec.

For instance, the apparent magnitude of the Sun is -26.74 due to its proximity to the Earth, while the actual or Absolute Magnitude is +4.83.

The absolute magnitude scale is normalised with reference to a distance of 10 parsecs. If we know both these the distance may be calculated using the "distance modulus" equation given by

$$m_\lambda - M_\lambda = 5\, log_{10}\, D - 5 = \, -5\, log_{10}\, p - 5 \qquad (1.4)$$

Here D is the distance in parsec and p the annual parallax in arcsec.

We can define also the bolometric magnitude representing the total integrated flux in all wavelengths given by

$$M_{bol} = 4.75 - 2.5 \log_{10}(L/L_\odot) \qquad (1.5)$$

where $L_{\odot}$ is the luminosity of the Sun and the value 4.75 is the bolometric magnitude of the Sun. The bolometric correction is defined as

$$BC = m_{bol} - m_{\lambda} = M_{bol} - M_{\lambda} \tag{1.6}$$

Objects appear small or point-like (of the order of arcsec or smaller) because they are single sources and far-off; they can appear big if they are bigger intrinsically (extended sources more than several arcsec to several degrees). At sufficiently large distances even the extended sources appear point-like. For **extended sources** (sizes more than a few arcsec in size) the magnitude scale usually refers to per square arcsec (the brightness of the object divided by its solid angle, (see Chapter 4).

1.1.7 Doppler Shift: Analogous to sound waves, light waves also undergo Doppler shift. For a celestial object moving in space with reference to an earth-based observer, the central wavelength/frequency (λ/ν) of a spectral line from the object shifts by an amount proportional to the velocity of the object (v). This is given by,

$$\frac{\Delta\lambda}{\lambda} = \frac{v}{c} = \frac{\Delta\nu}{\nu}$$

Here c is the velocity of light. If the object is receding from the observer, the frequency of the radiation decreases, or the wavelength increases, and such a shift is called a "red shift". Blue shift occurs when the object approaches observer.

1.2 A Glossary of Astronomical Objects

We present in this section a brief outline of characteristic features of various astronomical objects. This does not claim an exhaustive description; hence the reader may refer to more general books on astronomy for a comprehensive treatment. Over the past decades, there have been several excellent books written by eminent authors for general and specific topical reference on observational astronomy and theoretical astrophysics (e.g., Spitzer 1978; Lèna 1979; Dyson & Williams 1980; Shu 1982; Prialnik 2000; Whittet 2003; Smith 2004; Stahler & Palla 2004; Schulz 2005; Tielens 2005; Carroll & Ostlie 2007; Bradt 2008; Longair 2011; Sutton 2012; Lang 2013; Barbieri & Bertini 2020; Heidt 2022).

Figures 1.3 and 1.4 show images of the celestial sky mapped in the visible and infrared wavelength regions (see Longair 2011 for details). As may be made out from these images there appears a variety of objects in the sky:

stars, interstellar medium containing nebulae and molecular clouds and distant external galaxies. In the figures we can see bright regions of stars and emission nebulae as well as dark regions due to extinction by gas and dust. Such dark regions also reveal cold regions emitting in much longer wavelengths than visible and near-infrared wavelengths.

Astronomy and Astrophysics is the branch of Physical Science that strives to understand the origin, and evolution of various objects that constitute the celestial sky. Towards this goal, we need to understand these celestial objects in terms of the underlying physical processes. Therefore, Photometric and Spectroscopic investigations of various celestial objects become one of the most important aspects of observational Astrophysics. We give below short notes on celestial objects from solar system planets to external galaxies via stars and interstellar medium.

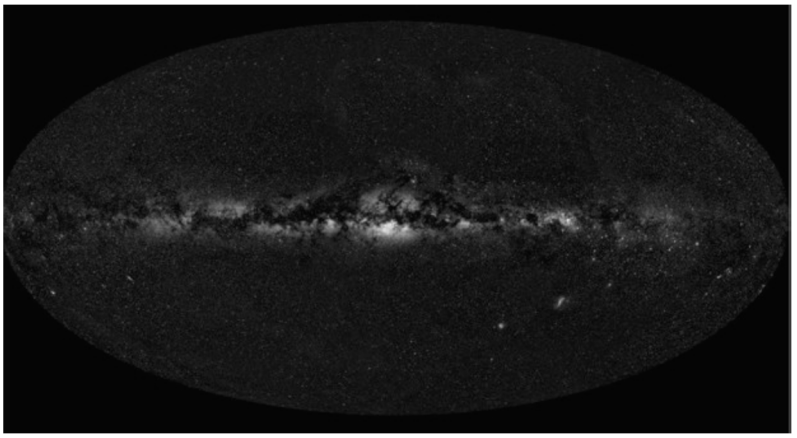

Figure 1.3: Celestial Sky seen in visible light (Longair 2011).

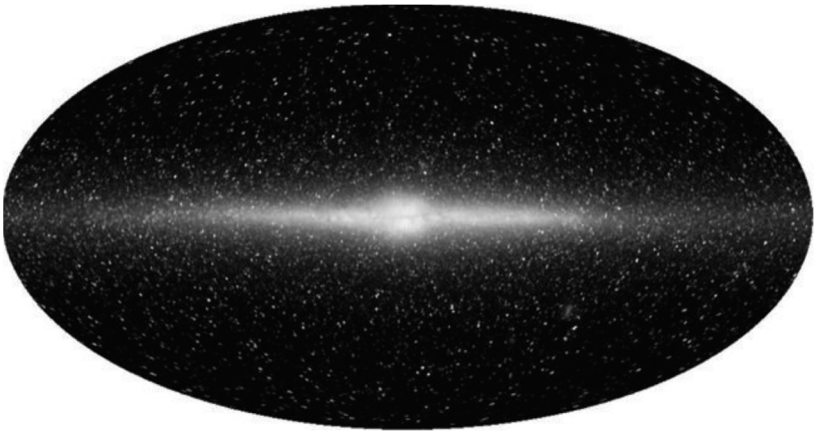

Figure 1.4: Celestial sky seen in near-infrared light (Longair 2011).

1.2.1 The Sun: The star of our solar system, the Sun, is a G2V type star. Due to its proximity to an Earth-bound observer, it is the only star that facilitates studies at an unprecedented spatial resolution (in terms of surface area covered per picture element) so that the regions of its photosphere regions were discerned into sub-regions such as chromosphere and corona. From this close-range, astronomers were able to identify unique phenomena such as spots, coronal emissions, coronal holes, coronal mass ejections, prominences, flares, plages, granules and super granules and spicules or filaments and so on. Therefore, the Solar studies have a bearing also on stars that are Sun-like. With the help of a great volume of multi-wavelength observations from both ground-based and space-based solar-telescopes, the physical phenomena responsible for the behaviour of the Sun have been primarily understood, although several issues remain unsolved. It is in its middle age in its main sequence phase. The star's age is estimated to be 4.57 x 10^9 years. The Sun has a radiative core and a convective envelope. Its magnetic field plays a major role in its evolution. Due to its magnetic field its tenuous atmosphere called corona is heated to a few million degrees K. The solar plasma also leads to a atomic and ionic excitation by collisions with electrons. The magnetic field also leads to generation of synchrotron radiation. For a comprehensive review of the Sun and Solar Physics we may refer to Aschwanden (2019).

Figure 1.5 illustrates the structure of the Sun in a schematic way. The central core where nuclear reactions occur is shown in dark with regions of radiative equilibrium and convective equilibrium are shown surrounding it respectively in grey. In the radiative region the energy transport to the upper layers is done predominantly by radiation. In the outermost convective region, the transport of energy is done by convection. In this region the solar magnetic field is also generated by the process called dynamo. The dynamo process itself is triggered by differential rotation in these layers. These regions are shown nearly in the relative proportion. The outer regions namely the photosphere, the Chromosphere and the Corona are shown in relative proportions but in comparison with the interior regions. Above the dark line (circle) where the optically thick region exists is the Sun's atmosphere. The effective temperature of the Sun refers to the equilibrium temperature of the photosphere, a very thin region of a few hundred kilometres. Above the photosphere occur the Chromosphere and a thin (of nearly a hundred kilometres thick) region called Transition region. Above the transition region is the Solar Corona (the outer boundary shown in the figure is only symbolic and not to scale in comparison with the lower layers of the Sun's atmosphere. The coronal plasma is called "the million-degree corona" energised purportedly by the dissipation of solar magnetic fields.

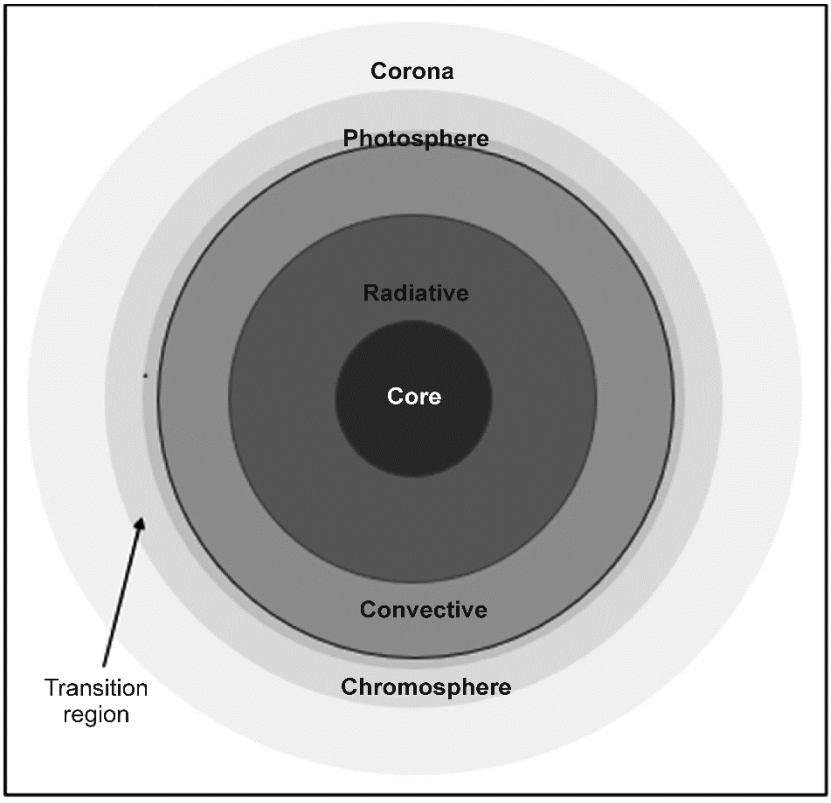

Figure 1.5: Solar structure shown schematically: the sizes from the core to photosphere are in relative proportion while those from photosphere outwards are separately in relative proportion.

1.2.2 Planets: Planets around stars, such as the Sun, are believed to be formed in the debris disk around protostars (or the proto-Sun in the case of the Solar system) by condensation of planetesimals or gravitational collapse before the disk is blown off by stellar winds and radiation pressure. A planetary body having a mass less than about 0.001 $M_{\odot}$ has only its potential energy converted to heat energy for its sustenance. It shines due to its albedo (reflected light) from the parent star. Sizes of planets vary from a fraction of Earth radius to a few times the size of the largest Solar system planet Jupiter. The distances from their parent star (the Sun for the Solar System) vary from a fraction of to several AU (astronomical unit). Table 1.2 gives some important parameters for Solar system planets. Without considering the effect of possible atmosphere of a planet, its effective dayside temperature due to heating by the parent star may be estimated from the radiation equilibrium equation (i.e., radiation absorbed equals radiation emitted) as follows:

$$T_P = T_S\,(R/2D)^{1/2}\,K \tag{1.7}$$

where T_S, and T_P are effective temperatures of the star of radius R, and its planet situated at a distance D. The above relation may be derived from a simple consideration that the absorbed radiation by the planet must be equal its emitted radiation. For the Solar System case this may be simply written as,

$$T_P = (1-A)^{1/4}\,\frac{278.3}{D(AU)^{0.5}}\,K \tag{1.8}$$

The solar effective temperature was taken as $T_{\odot} \sim 5770$ K and 1 AU = 1.4959 x 10^{11} m. The effect of the planetary (bond) albedo (A) is given by the factor $(1 - A)^{1/4}$. This will give a temperature of 255 K for Earth while the actual average surface temperature is 283-293 K. The difference may be attributed to the effects of the atmosphere of the earth.

Table 1.2 lists the effective temperatures of solar system planets (without Albedo factor) along with the albedo factors. For comparison, measured mean temperatures (T_M) are also listed. Also given in the table are, distances, masses (in terms of Earth mass, $M_{\oplus}$), average densities, orbital eccentricities and, inclinations of the eight planets. These data are from: http://nssdc.gsfc.nasa.gov/planetary.

Table 1.2: Solar System Planets – Physical Parameters.

Planet	Distance (AU)	Mass ($M_{\oplus}$)	Density ρ (gm/cc)	e	i deg	Albedo Factor $(1-A)^{1/4}$	T_P (K)	T_M (K)
Mercury	0.39	0.055	5.42	0.205	7.0	0.968	447	440
Venus	0.72	0.815	5.24	0.007	3.38	0.562	327	737
Earth	1.0	1	5.51	0.017	0	0.911	278	288
Mars	1.52	0.107	3.93	0.093	1.85	0.931	225	208
Jupiter	5.20	316.58	1.33	0.048	1.3	0.901	122	163
Saturn	9.57	95.14	0.69	0.054	2.48	0.901	90	133
Uranus	19.29	14.54	1.27	0.047	0.77	0.915	64	78
Neptune	30.24	17.08	1.64	0.009	1.77	0.918	51	73

1.2.2.1 Exoplanets: It is very reasonable to assume that stars other than the Sun may also host planets. The genesis for such observations came when the Infrared Astronomical Satellite (IRAS) with its discovery of the presence of large dust grains or planetesimals around main-sequence stars such as Vega, indicating that the debris (discs) around the stars formed during their formation stage may indeed become source of material to form planets (see e.g., Zuckerman 2001). Attempts were made to detect planets outside the

solar system during the last quarter of the 20th century. First successful detection of an extrasolar planet or simply "exoplanet" was made by Mayor & Queloz (1995) in the nearby star 51 Pegasi, using high-resolution spectroscopy. From Newtonian mechanics, we understand that a pair of a host star and its planet, forming a binary system, revolve around the centre of mass of the system. While the planet in the system makes a much larger orbit, the star makes a much smaller one around the centre of mass. For an Earth-bound observer, the periodic change in the position and velocity of rotation and the time of arrival of light from the parent/host star form the observables for the detection of a planet. Further the periodic dimming of light from the star in question can also be detected when its planet passes in front while orbiting. Due to the very large difference in the brightness of the star and that of a planet (amounting to typically about 9 orders of magnitude for Sun/Jupiter), it is very difficult to observe the planet directly by imaging. By using specially designed masks planets separated by 1 arcsec from its host star may be detected. Several space-borne photometers (for Kepler, see Howell et al 2014, for Transiting Exoplanet Survey Satellite (TESS), see Ricker et al 2016 and, for JWST, see Carter et al 2023) were flown to detect planets around nearby stars using transit technique. In order to estimate reliable masses of planets however the transit observations need complimentary/supplementary ground-based radial velocity observations using high resolution and high precision spectrometers. Masses of planets may also be determined using the gravitational lensing technique; such observations are however few and far between. One of the important criteria of whether an extrasolar planet may possibly be habitable is its surface temperature to be conducive for the existence of water in liquid phase. Using the host/parent star parameters, equivalent blackbody temperature of the planet may be estimated using the eqn. 1.8. Lately, attempts are being made to detect the planetary atmospheric composition as well using transit spectroscopy method. Such observations will also be useful in determining the habitability of exoplanets. For a comprehensive review of the detection and science of exoplanets we may refer to Kaltenegger (2017).

1.2.3 Stars: Stars constitute the most important components of a galaxy. They account for more than 90% of the mass and luminosity of a galaxy. The rest being from gas and dust. The formation and evolution of stars account for the chemical composition and evolution of a galaxy. Star formation and evolution are thus one of the most important problems of astrophysics. Stars are believed to form by gravitational collapse of denser parts of a molecular cloud caused by a perturbation in the interstellar medium (ISM) of a galaxy. During its contraction phase under its own gravity, a protostar (star in its formation stage) of sufficient mass attains temperatures of $T_c \geq$

$10^7 K$ at its core. At such high temperatures nuclear reactions take place involving hydrogen nuclei to form helium nuclei with the release of nuclear fusion energy. Masses less than about 0.08 $M_\odot$ cannot attain such high temperatures and end up as what are called Brown Dwarfs. These objects are however capable of burning deuterium at their cores for a brief period in their initial phases. The mass limit for Brown Dwarfs is 0.001 $M_\odot$ below which begins the planetary regime. Stars of different masses have different surface temperatures (and hence different spectra) and sizes. The higher the mass the higher will be its effective temperature and size and shorter will be its lifetime.

1.2.3.1 Classification of Stars: Stars are classified into various types based on their surface or effective temperatures (T_{eff}) or colours – from the hottest O type stars (T_{eff} around 3000 K) to the coolest M type stars (T_{eff} around 3000 K). The spectral types are designated by the letters O, B, A, F, G, K, M in the order of decreasing effective temperatures with sub-types within each type designated by numerals from 1 to 9; 1 being the hottest and 9 the coolest of the subgroup. For example, an O1 star is hotter than an O2 star and so on. Stars of cooler surfaces than M types, discovered lately, are called very low mass stars (VLM stars) and their spectral types are called L and T types (Kirkpatrick 2005). It is to be noted that this temperature or spectral classification is based on the so-called dwarf or main sequence phase during which stars remain stable with core hydrogen-burning as the energy source. We can understand the significance of the spectral classification (based on the surface or effective temperature of a star) from Fig 1.6. The figure shows the line strength (in arbitrary units) of different ionization stages of various important and abundant elements as a function of stellar (effective) temperature (hence the spectral type). We may notice that the hottest stars of O type show in their spectra He II (singly ionized Helium) and HeI (neutral Helium) lines (in absorption). The stars of spectral type A0 having a surface temperature of about 10000 K show predominantly the Hydrogen recombination lines in absorption. The cool stars (such as K0) show Ca II (singly ionized Calcium) absorption lines while still cooler stars (M types and even cooler stars) show molecular lines (such as TiO, VO) in their spectra. We may note here that Saha's thermal ionization equation gives the theoretical (physical) foundation for the spectra exhibited by stars of different colours. Table 1.3 gives some important parameters (in Solar units) for stars of different masses (spectral types) in the main sequence phase (these are mean parameters for dwarfs compiled by Pecaut & Mamajek 2013). A second type of classification called the luminosity classification is based on the evolutionary stages of stars (discussed below).

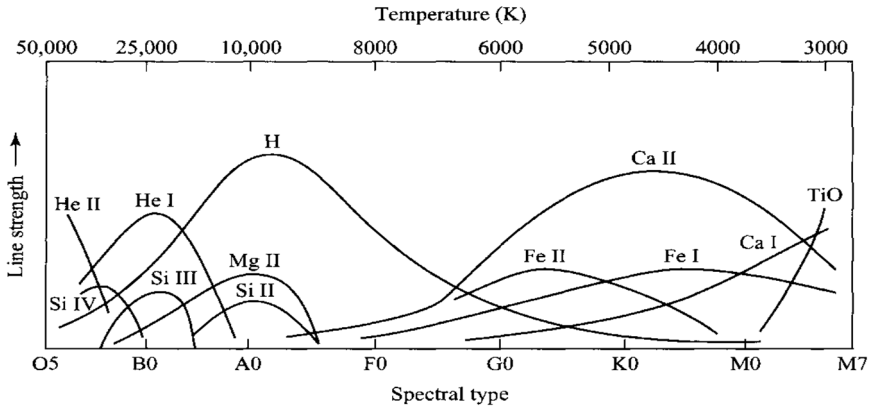

Figure 1.6: Ionization stages of abundant elements in stars of different effective temperatures or spectral classes (from Carroll & Ostlie 2007).

1.2.3.2 Main Sequence: The longest phase in the life of a star of any mass is known as the Main sequence. This phase is signified by nuclear reactions at the core of a star involving hydrogen nuclei (proton-proton or p-p chain) fusing to form Helium nuclei. Such stars also called dwarf stars in the luminosity classification. Stars of different masses make a sequential track in the luminosity-temperature space as shown in Fig 1.7. The time that a star spends in this phase depends up on its mass and luminosity, M/L. We notice that since L increases with M as $L \sim M^{3\text{-}4}$, the main sequence timescale decreases rapidly with increasing M: the smaller the mass the longer is the main sequence lifetime. The main sequence timescale may also be termed as nuclear timescale (see later sections of this chapter).

As mentioned above, stars spend most of their lifetimes in the hydrogen burning main sequence phase. After the exhaustion of hydrogen fuel at the core (which is now helium-rich), a star starts contracting under the inexorable pressure of gravity. This leads to the rise of the core temperature. The envelopes however are cooler and start to expand to maintain hydrostatic equilibrium thus making the star expand in size to become a Red Giant. The contracting core which is now predominantly helium-rich will eventually attain temperatures more than $\sim 10^8$ K. At this stage nuclear reactions will be rekindled fusing 3 or 4 helium nuclei to respectively synthesise carbon and oxygen nuclei. This stage lasts for much shorter timescales than the hydrogen burning main sequence stage. After the exhaustion of the helium the core becomes once again inactive, and the star sustains on the shell-burning – the helium shell surrounding the core and the outer hydrogen shell surrounding the latter. For most part of this stage, it is the hydrogen burning shell that supplies the fuel while helium shell accounts for about 10% of the time. During this alternate hydrogen-

helium burning cycles the star's envelope once again expands and becomes what is called an asymptotic giant branch star (AGB star). The luminosity of the star rises asymptotically with temperature. Now depending upon the initial mass of the star further nuclear reactions may take place at the core. For a star of initial mass typically less than about 8 $M_{\odot}$ the core remains inactive, and the envelopes keep expanding. These stars, called intermediate mass stars, eject their envelopes into the ISM as planetary nebulae (PN) while their cores cool down and eventually end up as White Dwarfs (WD).

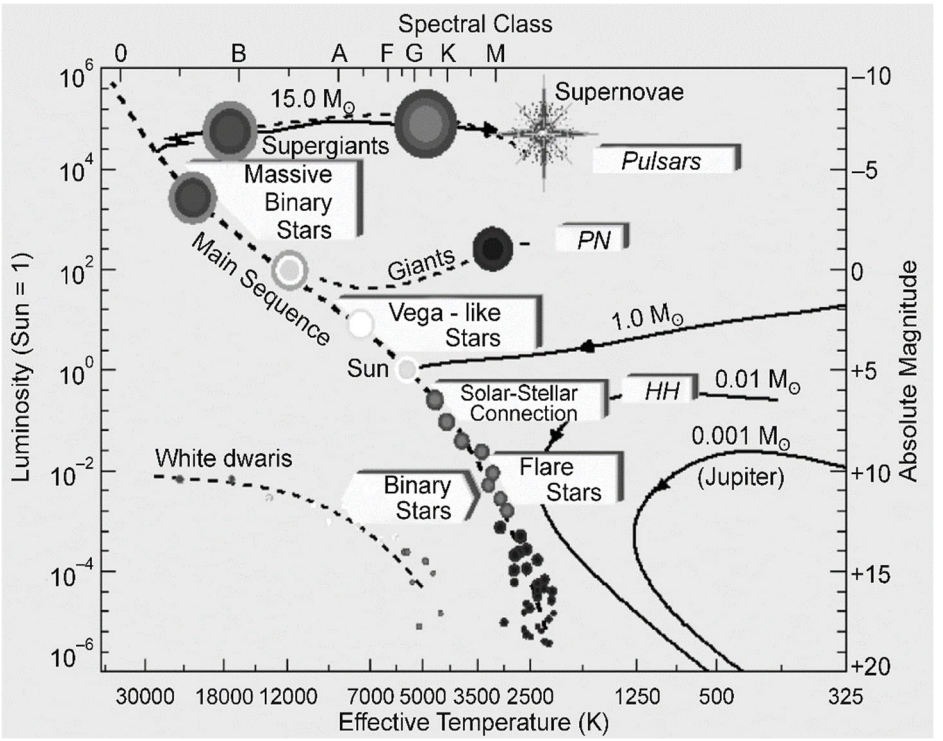

Figure 1.7: Herzsprung-Russell Diagram showing main sequence stars in the Effective Temperature- Luminosity plane. Also shown are various pre- and post-main sequence phases of stars (from G. Carenini - www.ca.ubc.ca).

Stars with masses larger than 8-10 $M_{\odot}$ carry forward the core nuclear activity. For stars having initial mass more than ~ 15 $M_{\odot}$, the core becomes predominantly an Iron core whence the nuclear fusion reactions cease to continue. At this stage, the star becomes unstable due to the onset of a series of fission reactions that are endothermic in nature (requiring energy). This leads to a catastrophic core collapse followed by energetic explosion. The resulting tenuous nebular object containing the ejected matter, rich of

heavy elements, is called a Supernova. Depending upon the core mass left behind the less massive core becomes a Neutron Star (NS) by contraction, while a more massive core becomes a Black Hole (BH) for the gravity finally becomes inexorable.

Table 1.3: Physical Parameters of Main Sequence Stars (Luminosity Class = V). Numbers in the parentheses are in powers of 10.

Sp. Type	T_{eff} (K)	L ($L_\odot$)	M_V (mag)	BC (mag)	M ($M_\odot$)	R ($R_\odot$)	τ_{ms} (10^6 yr)	τ_{KH} (10^6 yr)
O3	44900	6.6×10^5	-5.8	-4.01	59	13.4	0.89	0.01
O6	39500	2.3×10^5	-5.1	-3.57	35	10.3	1.50	0.02
B0	31400	4.5×10^4	-3.9	-2.99	17.7	7.16	3.95	0.03
B5	15700	5.9×10^2	-0.85	-1.34	4.7	3.36	80.0	0.35
A0	9700	38	0.99	-0.21	2.18	2.19	570	1.81
A5	8100	12.3	2.01	0.00	1.88	1.79	1.5(3)	5.0
F0	7220	7.24	2.57	0.01	1.61	1.73	2.2(3)	6.6
F5	6550	3.63	3.37	-0.02	1.33	1.47	3.7(3)	10.5
G0	5930	1.35	4.48	-0.065	1.06	1.1	7.8(3)	4.0
G5	5660	0.89	4.98	-0.105	0.98	0.97	1.1(4)	35.0
K0	5270	0.46	5.78	-0.195	0.88	0.81	1.9(4)	65.9
K5	4440	0.17	7.28	-0.63	0.70	0.70	4.1(4)	130
M0	3850	0.07	8.80	-1.15	0.57	0.59	8.1(4)	254
M5	3060	3×10^{-3}	14.15	-3.11	0.16	0.20	5.3(5)	1.4(3)
L0	2270	2×10^{-4}	20.0	-6.25	0.08	0.10	4.2(6)	1.1(4)
T2	1220	2×10^{-5}	-	-	0.06	0.10	3.0(7)	6.3(4)
Sun (G2)	**5770**	**1.0**	**4.80**	**-0.08**	**1.00**	**1.0**	**1.0(4)**	**31.7**

We notice that during the evolution beyond the main sequence stage stars tend to increase their sizes in order to maintain hydrostatic equilibrium. This process leads to increasing of their initial (main sequence) luminosities (recalling that luminosity is proportional to R^2 and T^4). Based on their evolutionary stage, further classification of stars, called the luminosity classification is made. This classification serves complementary to the colour-classification discussed earlier. Accordingly, the Luminosity Class I stars are called Super Giants; Class II and III are called Giants; Class IV are Sub-Giants and Class V are known as Dwarfs that represent the main sequence phase; Class VI are Sub-Dwarfs. For example, a G3 dwarf is designated as G3V, an F4 giant as F4III and an O5 super giant is denoted by O5I and so on. Fig 1.7 shows a useful depiction of stars of different masses and luminosity stages in the Temperature-Luminosity plane and such a

diagram is called Herzsprung-Russell diagram or H-R diagram. In this diagram stars in all stages of their lives may be depicted in the luminosity-temperature space – right from stars in making (protostars) to evolved giant stars through the hydrogen burning main sequence stars (see the Figure 1.7). The typical loci of luminosity classes of stars are shown clearly and separately in Fig 1.8 in the luminosity-temperature space – their evolution being from the dwarf (V class) stage towards right.

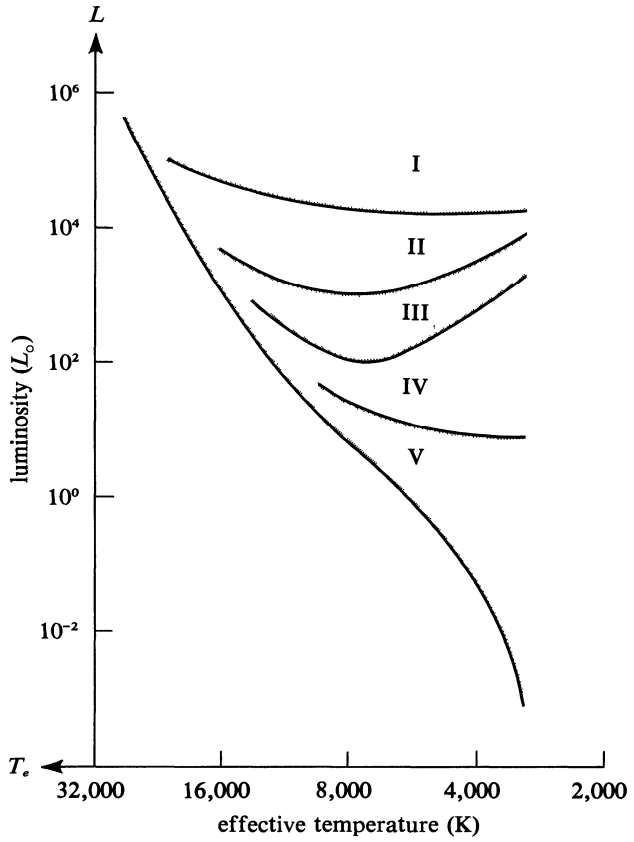

Figure 1.8: Luminosity Classes of Stars in the HR Diagram (Shu 1982).

1.2.3.3 Equations Governing the Stellar Interiors: The interiors of stars are basically governed by hydrostatic and thermal equilibria, the continuity (conservation) of mass and luminosity and finally, the energy release by nuclear reactions and the transport of this released energy to the surface layers either by convection or by radiation. The most important inputs to these equations are the initial mass and the elemental composition of the star, although magnetic field and rotation also may contribute significantly. Such a theoretical foundation allows us to understand the behaviour of the

fundamental parameters pertaining to the stability and evolution of stars – the variation of temperature, pressure, density and luminosity of matter from the core towards the surface. Firstly, it is important to establish the equation of state in the stellar interior which defines the relationship between the gas pressure and the temperature and density (see, for a detailed discussion, Prialnik 2000). For an ideal gas we have, $P = (\rho kT/\mu_m m_H)$, where T is the gas temperature, ρ is the pressure, μ_m is the mean molecular weight (determined by the composition of the gas) and m_H is the mass of a hydrogen atom. Without going into the details of their derivation we give below the equations governing the stars for reference:

$$\frac{dM_r}{dr} = 4\pi\rho_r r^2 \ \ (conservation\ of\ mass) \tag{1.9}$$

$$\frac{dP_r}{dr} = -\frac{G\rho_r M_r}{r^2} \ \ (hydrostatic\ equilibrium) \tag{1.10}$$

$$\frac{dL_r}{dr} = 4\pi\rho_r r^2 \varepsilon \ \ (continuity\ of\ luminosity) \tag{1.11}$$

$$\frac{dT_r}{dr} = -\frac{3\kappa\rho_r}{16\sigma T_r^3}\frac{L_r}{4\pi r^2} \ \ (radiative\ transport) \tag{1.12}$$

$$\frac{dT_r}{dr} = \frac{(\gamma-1)T_r}{\gamma P_r}\frac{dP_r}{dr} \ \ (convective\ transport) \tag{1.13}$$

In the above equations the temperature T_r, pressure P_r, mass density ρ_r and luminosity L_r are all functions of the radial distance r from the core centre to the surface of a star; ε is the rate per unit mass at which energy is produced from thermonuclear fusion reactions (such as the proton-proton (p-p) chain to convert H into He nuclei); κ is the mean opacity of the stellar layers; σ is the Stefan-Boltzmann constant; and γ is the adiabatic constant (ratio of heat capacities at constant pressure and constant volume). These equations are for a static situation since the time dependency is not considered. Time dependency would be of importance especially in the case of rapid phenomena such as the process leading to supernova explosion in massive stars and the pulsations of intermediate mass stars. For details of this topic, we may refer to the excellent book by Prialnik (2000).

1.2.3.4 Stability Criteria and Timescales of Stars: It is instructive to give important stability criteria and timescales of stars based on some of the above equations. We already introduced the timescale for hydrogen-burning stage called the main sequence timescale.

Dynamical Equilibrium: As mentioned before the interiors of stars are in hydrostatic equilibrium (eqn. 1.10) – the pressure gradient balancing the gravitational force against dynamical instability or collapse. It is given by.

$$\frac{dP_r}{dr} = -\rho \frac{GM_r}{r^2} \tag{1.14}$$

where P_r is the pressure (kinetic and radiation) and M_r is the mass of the star at a radial distance r from the centre and ρ is the average mass density. Situations arise during the life of a star when the equilibrium may be upset.

Chandrasekhar Limit: For a degenerate core, in which the gravitational contraction is countered by the degeneracy pressure of electrons or neutrons (in case of White Dwarfs or Neutron stars respectively), the limit on its mass above which it collapses under its own gravity is given by Chandrasekhar limit.

$$M_{Ch} = 5.83\, \mu_m^{-2}\, M_\odot \tag{1.15}$$

where μ_m is the mean molecular weight; in case of He, C, O cores its value is 2 and the limit reduces to 1.44 $M_\odot$. For a Fe core the limiting mass is 1.26 $M_\odot$. Masses above these limits would undergo inexorable gravitational collapse (see Prialnik 2000).

Eddington Limit for Luminosity: Eddington examined the case where radiation pressure alone balancing the gravitational pressure. Under this radiative equilibrium condition, the limit on the luminosity above which the star becomes unstable (leading to disruption) due to radiation pressure is evaluated by Eddington as

$$L_{Ed} = \frac{4\pi cGM}{\kappa} = 3.2 \times 10^4 \left(\frac{M}{M_\odot}\right)\left(\frac{\kappa_{es}}{\kappa}\right) L_\odot \tag{1.16}$$

where κ is the mean opacity which is a function of temperature and composition of the star, taken relative to the opacity due to electron scattering, κ_{es}. $L_\odot$ is the solar luminosity. The star loses its radiative equilibrium and disintegrates if its luminosity exceeds the Eddington limit (see Prialnik 2000).

Important Timescales: Based on the equations governing the interiors of a star we can define a few important timescales relevant to stellar physics.

Dynamical Timescale: As we have mentioned a star maintains a state of hydrostatic equilibrium by balancing of the inward pulling gravitational pressure with kinetic gas pressure. If there occurs at some of point of time an imbalance between the two competing forces, there would be a quick restoration of equilibrium within a short time. This is called the dynamical timescale (see Prialnik 2000). It may be derived approximately as the rate

of change of size of a star as a particle on its surface tries either to escape (with an escape velocity v_{esc}) or undergoes a free-fall (with a free-fall velocity v_{ff}). Thus,

$$\tau_{dyn} \approx \frac{R_*}{v_{esc}} \approx \frac{R_*}{v_{ff}} \approx \frac{1}{\sqrt{G\rho}} \approx 1000 \left[\frac{R}{R_\odot}\right]^{3/2} \left[\frac{M_\odot}{M}\right]^{1/2} sec \qquad (1.17)$$

where G is the gravitational constant and ρ the average mass density of the star under consideration. For the case of the Sun the dynamical timescale is ~ 1000 sec, while for a O3V star it is about 6 days.

Thermal/Kelvin-Helmholtz Timescale: Another timescale of importance is that at which the star's internal energy arising due to gravitational contraction is expended by emission of radiation. This is given by.

$$\tau_{th} \approx \frac{U}{L} \approx \frac{GM^2}{R\,L} \approx 3.17 \times 10^7 \left[\frac{M}{M_\odot}\right]^2 \left[\frac{R_\odot}{R}\right] \left[\frac{L_\odot}{L}\right] yrs. \qquad (1.18)$$

For the Sun's case the timescale is approximately equal to $3x10^7$ yrs. This is the same as the familiar Kelvin-Helmholtz timescale (τ_{KH}) on which the gravitational contraction raises the core temperature and density of a star to the values conducive for the onset of the hydrogen-burning nuclear reactions. This timescale also defines the time taken by a star (of mass M) to reach the onset of main sequence phase or the zero-age main sequence (ZAMS) phase (see Zinnecker & Yorke (2007), for τ_{KH} as a function of $M_\odot$, $R_\odot$, and $L_\odot$). Essentially, we understand that a star must maintain both hydrostatic and thermal equilibrium for its stability against phases of expansion (leading to cooling) and contraction (leading to heating). Table 1.3 lists the thermal timescales for stars of various masses (from models of Schaller et al 1992; Pecaut & Mamajek 2013).

Nuclear Timescale: The theory of stellar interiors predicts that the core of a star is hot enough to trigger nuclear fusion reaction in which four hydrogen nuclei (protons) fuse to convert into one helium nucleus. Nuclear energy source is thus necessary and sufficient for the star to sustain on timescales that are estimated in the case of the solar system age which are very much longer than the K-H timescales.

The timescale that a core of certain mass completely converts itself from hydrogen dominated one to helium dominated one defines the nuclear timescale or the main sequence timescale. Here in this case the energy source is the nuclear energy at the core and is given by the Einstein's well-known equation $E=Mc^2$ and if the luminosity pertaining to this is L_{nuc} or L, then the timescale is simply given by (with ε as a constant that depends on the binding energy of a nucleon divided by its rest mass energy),

$$\tau_{nuc} \approx \frac{\varepsilon Mc^2}{L} \approx \varepsilon\, 4.5 \times 10^{20} \left[\frac{M}{M_\odot}\right] \left[\frac{L_\odot}{L}\right] sec. \quad (1.19)$$

Since the luminosity is a function of mass of a star the timescale becomes a very strong function of mass (related inversely). Again, for comparison for the case of the Sun this timescale is about 9 billion years (nearly the age of the Universe!). For more massive stars the times come down rapidly.

Adopting a value of $\varepsilon \sim 10^{-3}$, we obtain the nuclear timescale (which is orders of magnitude longer for Hydrogen burning cores than Helium cores) or the main sequence lifetime of a star in terms of years as

$$\tau_{nuc} \sim 1 \times 10^{10} \left(\frac{M}{M_\odot}\right)\left(\frac{L_\odot}{L}\right) yrs. \quad (1.20)$$

Table 1.3 lists main sequence or nuclear timescales for stars of various masses (taken from the models of Schaller et al 1992; Pecaut & Mamajek 2013).

A comparison of the three timescales as defined above gives us the inequality, valid for stars of all mass ranges, as

$$\tau_{dyn} \ll \tau_{th} \ll \tau_{nuc} \quad (1.21)$$

Thus, stars adjust themselves to changes in temperature and pressure on dynamical timescales of the order of hours at the maximum much shorter than the thermal and nuclear timescales. The thermal timescale determines the time required to attain core temperatures needed for the onset of nuclear reactions while the nuclear timescales represent the lifetimes of stars.

1.2.3.5 Stellar Evolution: For the sake of completeness and continuity, we give here a short rudimentary account of stellar evolution. As we have seen, stars spend a major part of their lifetimes in the main sequence stage, signified by the core-hydrogen burning. The higher the mass of a star the shorter its lifetime will be. Following the exhaustion of hydrogen, due to the absence of any energy source, the core undergoes a contraction while the envelope expands to maintain the hydrostatic equilibrium. This is the state when the star enters the red giant branch. The ongoing contraction heats up the core leading to the attainment of higher temperatures ($> 10^8$ K) triggering the nuclear reactions involving helium nuclei. These reactions, called the triple alpha processes, synthesize carbon and oxygen nuclei in the core. We note here that stars of masses less than 0.8 $M_\odot$ end up with degenerate helium cores, but in nature we do not find these (except those

evolved from binary stars), for the main sequence lifetime of a single star of such a mass is much longer than the time of universe or Hubble time (see Table 1.3). In stars of masses more than 0.8 $M_{\odot}$, after the exhaustion of core helium, once again, the contraction-expansion cycle starts. It is important to note that for stars of masses between 0.8 and 2.25 $M_{\odot}$ the cores become electron-degenerate before helium ignition starts leading to a runaway core-helium flash (Iben 1974, 1985; Prialnik 2000). The inactive core of the star has now hydrogen and helium shells burning alternatively providing energy for the star. For stars of masses less than 8 - 10 $M_{\odot}$, the core remains unignited, as the electron degeneracy pressure supports it from gravitational collapse. Their cores, initially very hot, will cool down to become white dwarfs, while their envelopes, ionized and excited by the central hot core, become planetary nebulae. For stars having masses more than 10 $M_{\odot}$, however, the ignition of successive cores will continue (beyond C-O) with heavier nuclei, till it reaches the stage of having a core of iron (Prialnik 2000; Langer 2012). At this stage, fusion reactions are no longer possible. The iron core will undergo a collapse following a series of endothermic nuclear fission reactions. This is followed immediately by a catastrophic highly energetic explosion called supernova (type II supernova). The degenerate cores of high mass stars will become neutron stars or black holes, depending upon their core masses. Thus, stars of all masses lose a major portion of their mass, and this mass loss enriches the surrounding medium called the interstellar medium and provides matter for the formation of next generation of stars.

1.2.3.6 Binary Stars: It is certainly possible and highly probable that stars mostly occur in binaries (for understanding origin of binaries, see Tohline 2002). It is estimated theoretically that more than 60% of the stars may have companions (see e.g., Iben 1985). Evolution of such a composite system of double stars is significantly different from that of a single star. This is due to the gravitational or tidal interaction between the two stars in the system affecting their dense extended atmospheres generated by mass loss during evolution beyond main sequence. We know that a star of higher mass evolves faster than the one that has a lower mass. Such a situation where the components of binary stars have different evolutionary timescales is highly dynamic. This leads to very interesting and often exotic possibilities arising in binary stellar systems.

Shown in Fig 1.9 is a schematic representation of a binary system in its composite gravitational field potential. The stars of masses M_1 and M_2 are shown as dark spots in the figure. The solid circles and dashed contours show the cross-sections of the iso-potential surfaces for the binary system:

the solid curves representing envelopes around individual components and the dashed curves the envelopes that are common for both the stars. The masses considered for the stars are nearly equal and hence the contours for each star look nearly the same. The two lobes (shown as solid contours) called the Roche lobes represent the two zero-gravitational potential surface regimes corresponding to the two stars. Within these lobes each star would govern the dynamics of a test particle. The point at which the two lobes meet is called the first Lagrangean point or L_1. Exactly at L_1 a test particle is floating in space freely being inside a potential well (or minimum). Four more such minima exist in the system as shown in the figure, called the Lagrangean points, L_2, L_3, L_4, and L_5. When the more massive star of the binary evolves (faster than its companion) it undergoes mass loss leading to filling of its own Roche lobe. The pressure at L_1 due to this filling ushers the matter into the Roche lobe corresponding to the second star of lower mass. The mass thus gained by the second star creates a hot spot on its surface as shown in Fig 1.10 and starts heating the surface matter. This situation, occurring in close-binary star systems, potentially changes the course of evolution of not only the receptor star but also the donor star (see e.g., Iben 1985; Marchant & Bodensteiner 2024). Their evolution would be very different from that of a single star of similar mass. Even intermediate mass stars in binary could end up as neutron stars or even black holes. Further, for instance in the general class of cataclysmic variable stars (see Warner 1995; Smith 2006), this type of mass transfer takes place in a binary system in which one of the stars (being more massive to start with) evolved into a white dwarf having lost the envelopes to the inter-binary or interstellar medium, the subsequent mass loss from the evolving secondary star (less massive to begin with) would lead to an explosive situation of rekindled nuclear reactions by CNO cycle on the surface of the white dwarf. This triggers a runaway of radiation transport. Such catastrophic situations lead to sudden brightening of the system known as Classical Nova (new star) phenomenon (see e.g., Chomiuk et al 2021). The situation may also lead (depending upon the masses of the stars) to what is known as a Type I supernova phenomenon. More massive stars in binary systems evolve into more exotic objects such as Low Mass X-ray Binaries and High Mass X-ray Binaries (LMXB and HMXB) in which the accreting components are believed to be neutron stars or black holes (for details on evolution of massive binary stars, see Marchant & Bodensteiner 2024). We may refer to excellent articles by Iben (1974, 1985) on the evolution of a single star and that of a binary.

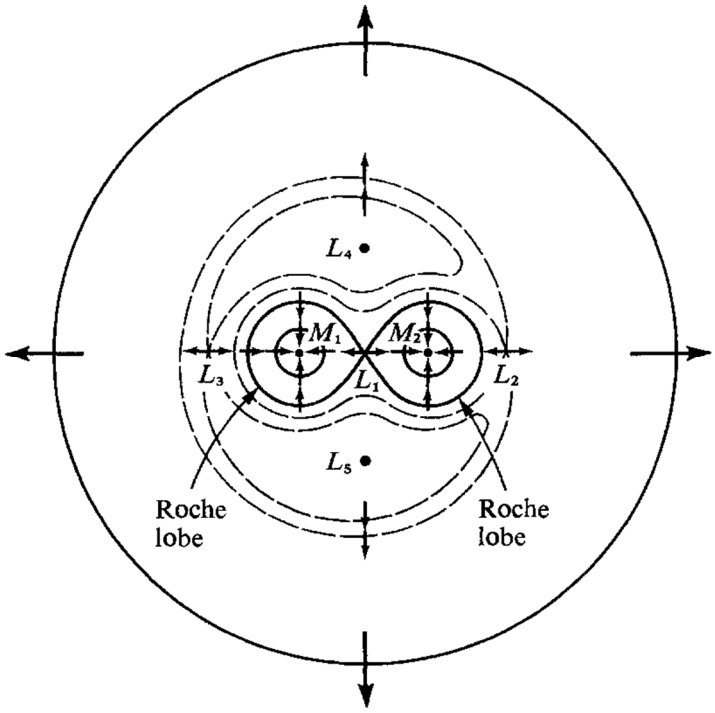

Figure 1.9: Gravitational iso-potential curves for a binary system of stars. The mass transfer takes place through the Lagrangean point L_1. The Roche lobes indicate the individual gravitational regimes of the two stars (from Shu 1982).

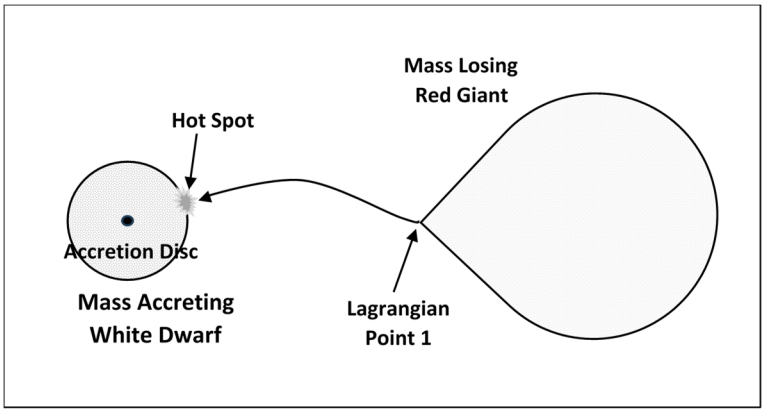

Figure 1.10: Mass transfer through L1 in a binary star – consisting of a compact object evolved from an initially more massive star and the currently evolving lower mass companion. The presence of the compact object may be inferred from energetic radiation emanating from the accretion disk since the cooler star cannot account for it (adapted from Shu 1982).

1.2.3.7 Mass Loss from Stars: Spectra of stars in main sequence phase show predominantly absorption lines from various constituent elements (such as H, He, Mg, Ca, Fe) in their envelopes against the source of hot inner regions (see Fig 1.6 and the right top panel in Fig 1.11). Cooler stars in the main sequence, in contrast, exhibit molecular absorption lines (such as TiO, VO). Spectral lines arising from the atmospheres of stars not only reveal the physical parameters but also the physical conditions of the star: whether the star is in the main sequence phase or has evolved into the giant phase and so on. Spectra can also identify the pre-main sequence phase of protostars as opposed to evolved stars.

Stars lose mass at different stages of their lives, particularly and predominantly after the main sequence phase. While in the main sequence phase stars lose mass at a very low rate (typically $< 10^{-12}\,M_{\odot}/yr$) by way of highly tenuous stellar wind, the mass loss rate increases dramatically by several orders of magnitude following the onset of the giant phase in the case of low and intermediate mass stars (see van Winkel 2003; Herwig 2005). When stars evolve into the giant stages copious mass loss occurs causing extended tenuous atmospheres normally called circumstellar regions. The line profiles from such stars appear a bit more complex than those from main sequence stars. Further, stars which are in the process of formation also possess circumstellar matter; the major difference in their case is that the matter is being accreted rather than ejected as in the case of evolved stars. The question of whether matter is ejected (in evolved stars) or accreted (in protostars) may be answered by spectroscopic and photometric observations.

Mass loss rate at a radial distance r from the star of mass M where the average density is $\rho(r)$ and the wind has reached its terminal velocity v_{∞}, may be given by,

$$\frac{dM}{dt} = 4\pi r^2 \rho(r) v_{\infty} \tag{1.22}$$

During the red-giant stage (following the exhaustion of core hydrogen nuclear fuel), stars lose mass at a rate of $10^{-9}\ M_{\odot}/yr$ while during their asymptotic giant branch stage (second red-giant stage after helium exhaustion at the core) the mass loss rate is as high as $10^{-6}\ M_{\odot}/yr$. Such a heavy mass loss leads to obscuration of visible light from the stellar photosphere due to large extinction. Stars are observable only in the longer wavelengths during these giant stages especially for cooler stars.

Massive stars of mass more than ~ 8-10 $M_{\odot}$ also lose most of their mass during the onset of supernova phase leaving behind cores that evolve to become neutron stars or black holes (see Vink 2022). In the case of binary

stars, the common envelopes contribute to mass loss (see e.g., Taam & Sandquist 2000). In the case of nova phenomenon, the surface matter of the accreting component contributes to the mass loss. Spectral lines arise from the tenuous gaseous matter thus ejected from these scenarios and typically help the observer unravel the underlying physical processes.

P Cygni Line Profiles: Several hot stars exhibit peculiar line profiles indicative of mass loss or wind - a combination of both absorption and emission lines known as P Cygni profiles. These are a result of blue-shifted absorption from out-flowing wind.

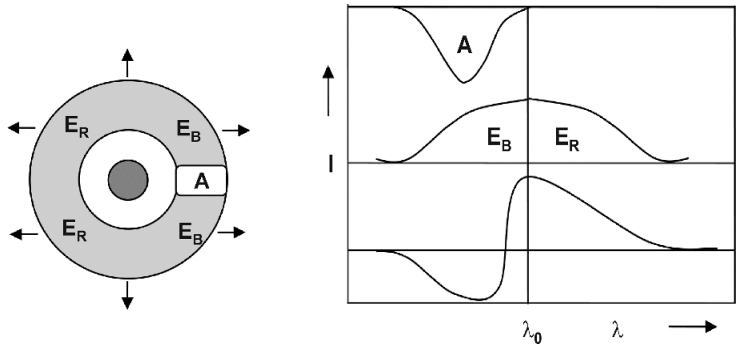

Figure 1.11: P Cygnii Profile formation. The patch A in front of the star accounts for the absorption profile (shown on top panel of the schematic graph on the right; the emission blue and red components are depicted in the middle panel and the resultant profile called P Cygnii profile is shown in the bottom panel.

As illustrated in Fig. 1.11 the star at the centre (which is either in a pre-main sequence or post-main sequence stage) is surrounded by a presumably spherical shell of matter colder than the stellar surface or the photosphere.

Under these conditions an observer would record an absorption profile of a spectral line from a given atom or molecule as shown in the right-side part of the figure marked A. This is the result of matter directly in front of the star (shown in grey in the left part of the figure) absorbing the radiation emanating from the hotter stellar photosphere; blue-shifted for an observer in front of the absorbing matter. The atoms/molecules present in the other regions of the circumstellar matter would also emit due to the excitation by either collisions or by radiation from the central star. These emitting regions are marked E_B and E_R for blue and redshifted regions respectively. The emission profile thus formed is shown in the middle panel of the right-side figure. The resultant of the two profiles, viz. the blue-shifted absorption profile and the emission profile symmetric about the rest wavelength as shown in the bottom panel of the right-side figure, is known as a “P Cygni

profile". Such a phenomenon was first observed in the case of the star P Cygni, a pre-main sequence star and hence the name. As mentioned already the P Cygni line profile has a typically shallow absorption line followed by a steep rising emission part that slowly tapers off towards the redshifted side of the spectrum as shown in the schematic figure. A star that accretes matter (such as a proto-stellar object) shows the absorption part in the redshifted part and such a profile is called an "inverse-P-Cygni" profile. For a detailed treatment of P Cygni profile formation, we may refer to Lamers & Cassinelli (1999).

1.2.3.8 Variable Stars: Stars exhibit variability in their overall light output and even their spectral line strengths in various stages of their evolution as well as during their formation stages. These are termed as intrinsic variable stars. Stars may also vary due to extraneous factors for instance due to occultation by another astronomical source such as a binary component or a planet. Such stars are called extrinsic variable stars. Variability may be periodic as well as aperiodic or quasi-periodic in both single and binary stars. For a general description of variable stars, we may refer to Percy (2007).

Periodic variability occurs in single stars mainly during their evolution into giant stages wherein they undergo periodic oscillations whose period depends upon the average density. In this category are the RR Lyrae variables having variability periods of a few hours, Cepheid variables with periods of a few days to a few tens of days and Mira variables having periods of a hundred to a few hundred days. RR Lyrae variables exhibit change in light output of 1 magnitude while the Cepheid variables show a linear relationship between their period and the magnitude of variability. These are examples of stars showing variability due to oscillations of their interior regions. Single stars also exhibit aperiodic variability during mass loss episodes.

It may be noted here that the discovery of the period-luminosity (or absolute magnitude) relationship discovered in Cepheid variables (by Henrietta Leavitt in the beginning of the last century) established a distance candle in the form of these stars for measuring distances to galaxies (we can see farther into the universe since these stars are bright enough to take us as far as the Virgo cluster galaxies).

Binary stars exhibit periodic variability due to the mutual obscuration of the binary components. Periodic changes occur in their spectral lines as well – single-line wherein only one of the two components exhibits spectral lines and double-line wherein both the binary components exhibit. Double stars also show variability due to mass loss or mass exchange between the two components. This includes the phenomena of Novae (and Supernovae)

which exhibit aperiodic variability in both their photometric output as well as their spectral characteristics over a period of a few weeks or longer (see recent review of Chomiuk et al 2021).

Monitoring of variable stars in both multi-band photometry and spectroscopy gives valuable inputs on the processes leading to such behaviour.

1.2.4 Interstellar Medium (ISM): The medium or matter between the stars in a galaxy is in general termed as interstellar medium or interstellar matter (ISM; for details on the topic, see Tielens 2005). The matter between stars is generally very tenuous but there exist regions of cold matter of high density. The temperature and density in ISM vary largely from one region to the other. The ISM comprises of gaseous and diffuse nebulae that are remnants from evolved stars including planetary nebulae, ejecta from intermediate mass stars having masses 1-8 $M_{\odot}$, supernova remnants, ejecta from Supernova explosion from massive stars with masses $> 15\ M_{\odot}$ and giant molecular clouds, containing gas and dust grains, that are sites of new star formation. Depending on the regional physical parameters, in particular the density and temperature, the ISM is divided into 5 main phases – (i) hot tenuous ionized regions; (ii) warm ionized regions; (iii) warm neutral regions; (iv) cold neutral regions and (v) cold molecular cloud regions. Each of these regions of ISM is distinct and distinguishable by its physical parameters such as the kinetic temperature and the density. Table 1.4 (data from Smith 2004) lists these phases along with their typical physical parameters.

Owing to the constituent gas and dust grains, the ISM absorbs/scatters the light from bright sources such as stars and makes them appear fainter for an observer. Dust grain formation takes place in ISM due to coagulations of matter in the cold environments. The gas molecules and dust particles scatter and absorb radiation from the hot sources contributing to the extinction of light along the line of sight for an observer.

The cold and visually dark regions of giant molecular clouds are the sites of star formation. The hotter regions such as the supernova remnants and planetary nebulae on the other hand indicate the presence of evolved stars that are losing or have lost mass back into the ISM. Thus, there exists such a cyclic phenomenon that is relentlessly recurring within the ISM. Since the stars are cauldrons of nuclear reactions, with every generation of stars the metallic content (elements heavier than Hydrogen and Helium) increases. This in turn changes the chemical composition of ISM itself and hence that of its host galaxy.

Fig 1.12 (adapted from Whittet, 2003) shows the phases of ISM in gas temperature – density space. We can see the large range of objects that constitute ISM from hot tenuous inter-cloud medium to cold dense molecular clouds. The lines that bound the marked regions show linear trend that maintains the pressure equilibrium between various phases (see Whittet (2003) for more details). Essentially the ISM gas pressure is given by $p = nkT$ with n and T denoting the number density and temperature and k the Boltzmann constant. If pressure were to be in equilibrium, nT (approximately equal to 3 x 10^9 m^{-3} K: from Mathis 2000) must be invariant or n should be inversely proportional to T. This is what the figure indicates. The equilibrium temperature is determined by the balance between heating and cooling processes (Spitzer 1978). The two main constituents of ISM namely the gas and the dust are heated by absorption of energetic photons from the interstellar radiation field or collisions with cosmic rays. The dust grains thus heated would cool by emitting photons at longer wavelengths (by the so-called reprocessing). The gas atoms and molecules not only absorb photons but also get heated up by collisions with photoelectrons from small dust grains; and the cooling mechanism is by emission of spectral lines.

Table 1.4: Phases of Interstellar Medium.

Phases of ISM	T (K)	n (m^{-3})	M ($10^9 M_\odot$)	Size (pc)	Object
Hot Ionized	3-20x10^5	3x10^3	0.003	10^3	SNR
Warm Ionized	10^4	3x10^5	0.05	10^3	PNe
Warm Neutral	8000	4x10^5	0.20	100	PDR
Cold Neutral	40-100	6x10^7	3.0	10	GMC
Molecular	3-20	3x10^8	3.0	1	GMC

We note here that the region marked 'HII region' representing the ionized Hydrogen region does not fall in this equilibrium regime. Other factors especially, the interstellar magnetic field also plays a role depending upon the ratio of kinetic pressure to magnetic pressure p_B ($\beta = p/p_B$ with $p_B \sim B^2$, where B is the Magnetic flux density). Magnetic field effects become significant in ionized or partially ionized regions. Turbulence also helps in keeping the regions dynamic and hence the equilibrium situation (as the figure seems to suggest) is rather an ideal one (Elmegreen 1997).

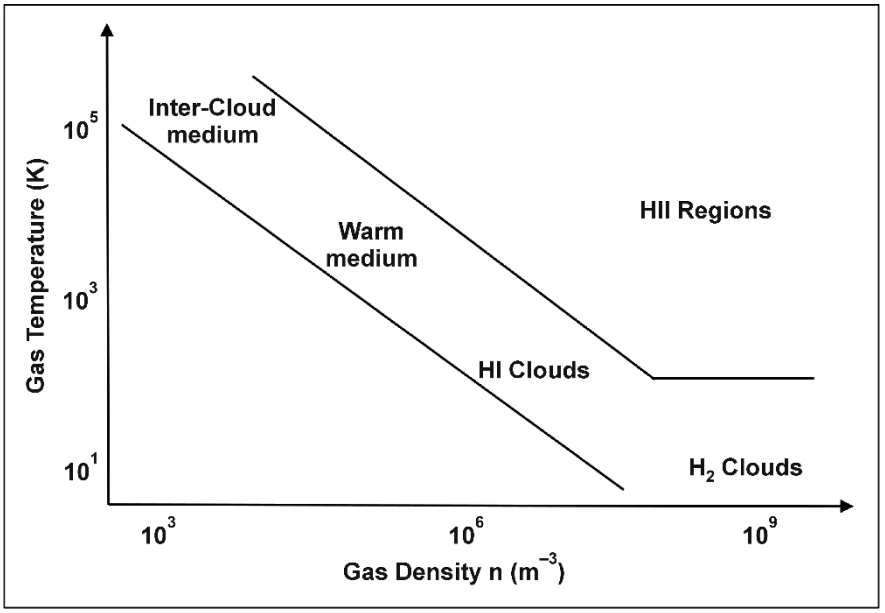

Figure 1.12: Interstellar Medium - temperature versus density for different phases (from Whittet 2003).

1.2.4.1 Star Forming Regions: Stars are believed to form from the small molecular clouds and the giant molecular clouds in the ISM. When a molecular cloud is perturbed by a disturbance such as a passage of supernova wind or AGB star wind, gravitational instability would set in breaking up the cloud into several smaller entities of higher density compared to their surrounding medium. In general, as a consequence of the Virial theorem under static equilibrium conditions (see e.g., Carroll & Ostlie 2007), we expect the following relation between various competing forces, namely the gravitational force acting towards the centre countered by the force due to kinetic pressure and that due to magnetic field,

$$2\{(KE)_p - (KE)_s\} + B + W = 0 \qquad (1.23)$$

where the first term in the equation gives the kinetic energy of the cloud in excess of that of background cloud with $(KE)_p$ and $(KE)_s$ representing kinetic energy of cloud and in the medium surrounding it respectively. The second term B represents the magnetic energy and the last term W the gravitational potential energy. If we drop the magnetic force term in the above equation, the static Virial theorem suggests that the total kinetic energy of the cloud is equal to half of the potential energy due to its gravitational force. Overcoming the gravitational force to establish a hydrostatic equilibrium calls for certain limits on the temperature and mass

density of the cloud. Now under certain special cases let us look at some important timescales.

Free-fall timescale: If gravity is the only force relevant, then the particles in a cloud experience a free-fall. The timescale of the free-fall can be obtained from the balance equation (1.23) as

$$\tau_{ff} = \left\{\frac{3\pi}{32G\rho_0}\right\}^{1/2} \tag{1.24}$$

where ρ_0 is the initial mass density of the collapsing object under its own gravity and G is the Newton's gravitation constant. Note that the free-fall timescale depends only on density irrespective of the initial mass of the collapsing cloud. For a typical average density in giant molecular clouds (GMC) of ~ 100 cm^{-3} we get the free-fall timescale of $\sim 10^7$ yrs.

Kelvin-Helmholtz timescale: As discussed earlier, this timescale indicates the timescale over which the gravitational energy alone can sustain the luminosity of the star. During this time, the central core temperature attains values more than 10^7 K at which stage nuclear fusion reactions involving Hydrogen nuclei are triggered. We can therefore interpret this timescale as the time taken by an object of mass M to reach the hydrogen burning stage or zero-age main sequence (ZAMS) stage.

Massive stars (with masses much more than the mass of the Sun) have the KH timescales (about 10^4 yrs for a collapsing cloud of mass enough to make an O type star) much shorter than their free-fall timescales and reach ZAMS stage even as the accretion is still on-going. This is in stark contrast with the formation of Sun-like or intermediate-mass stars. Let us recall that for the Sun, for instance, the K-H timescale is 30 million years. This difference in the K-H timescale is a major factor in deciding the processes leading to the formation of massive stars as opposed to the formation of low-mass or the Sun-like stars.

If only the kinetic energy term is considered to counter the gravitational potential energy, then we can derive a limiting mass above which the cloud becomes unstable against gravity and collapses. This exercise was first done by Sir James Jeans nearly a century ago when he considered the stability in a molecular cloud region subjected to a small perturbation and derived a limiting (perturbation) wavelength called Jeans length above which gravity prevails over kinetic pressure and the region collapses under its own gravity separating itself from its surroundings. The limiting wavelength is given by (see Smith 2004, for details)

$$\lambda_J = \left(\frac{\pi c_s^2}{G\rho}\right)^{1/2} \tag{1.25}$$

In the above equation c_s is the local sound speed and ρ the average mass density of the region under consideration. We can now use this length to evaluate the mass of the region under perturbation as (with temperature T in degrees Kelvin and particle number density n in m^{-3}),

$$M_J = \left(\frac{4\pi}{3}\right)\left(\frac{\lambda}{2}\right)^3 \rho \;=\; 1.18 \times \left(\frac{T}{10}\right)^{3/2} \left(\frac{n}{10^{11}}\right)^{-1/2} M_\odot \tag{1.26}$$

This limiting mass above which the cloud becomes unstable to perturbation is known as the Jeans mass.

When magnetic field is considered separately in the balance equation given earlier, we may derive the corresponding magnetic critical mass for a spherical cloud as (see Smith 2004)

$$M_\phi \;=\; 0.17 \frac{\phi}{G^{1/2}} \tag{1.27}$$

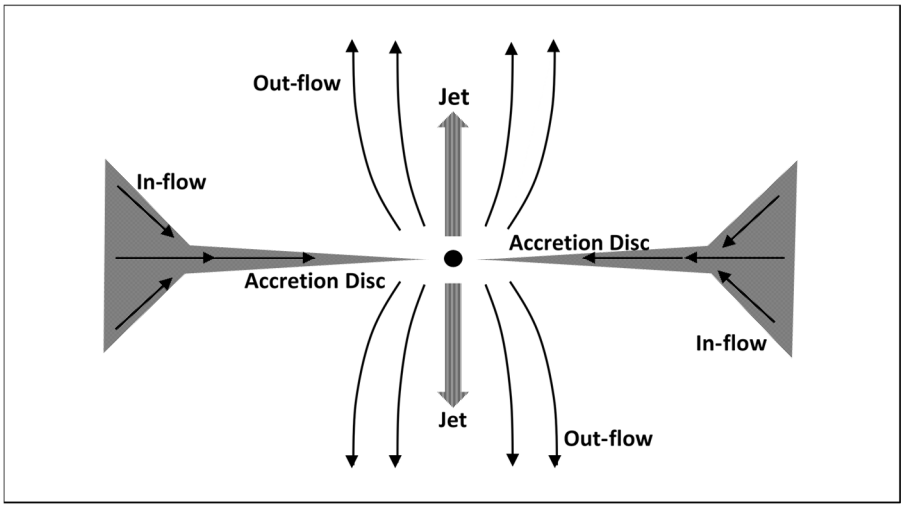

Figure 1.13: Structure of a protostar showing an accretion disk, outflows, and jets (adapted from Zinnecker & Yorke 2007).

where φ is the magnetic flux ($= \pi R^2 B$ with B as the magnetic field and R the size of the cloud). We may write the ratio of cloud mass to the magnetic critical mass as follows:

$$\frac{M}{M_\Phi} = 4.6 \times 10^4 \left(\frac{N}{10^{22}\, cm^{-2}}\right)^3 \left(\frac{B}{10^{-6} Gauss}\right)^{-3} \tag{1.28}$$

In the above equation $N$is the column density of Hydrogen nucleons (see Smith 2004). It gives an extremely high critical mass for magnetic support at large scales of cloud size.

We can now write down the modified Jeans critical length (considering both kinetic and magnetic forces separately and adding) as

$$\lambda_{JM} = \frac{3GM}{\pi\sigma^2}\left\{1 - \left(\frac{M_\phi}{M}\right)^2\right\} \tag{1.29}$$

where $\sigma$is the velocity dispersion or line width. This defines the critical size of the cloud that would collapse when compressed. Depending upon the strength of magnetic field we can have two cases – sub-critical case where magnetic field is strong in which the cloud would never collapse and super-critical case where magnetic field is weak in which the cloud would collapse. This latter case is believed to be the process by which high mass stars are formed: at larger sizes the molecular clouds are super-critical since the weak magnetic field fails to provide support the cloud against gravitational collapse. At smaller sizes the clouds may be sub-critical with strong magnetic field supporting the cloud against gravity; unless the effect of strong magnetic field is alleviated by the process called "ambipolar diffusion" (ion-drag due to strong neutral-ion bonding by collisions). It is not clear observationally as to the formation of star formation in sub-critical case. We may refer to Smith (2004) for an excellent treatment of the subject. The observable manifestations of a protostar, namely jets and accretion disk, are schematically shown in Fig 1.13 (adapted from Zinnecker & York 2007). Fig 1.14 shows these structures in a young stellar object (YSO), observed in various diagnostic spectral lines.

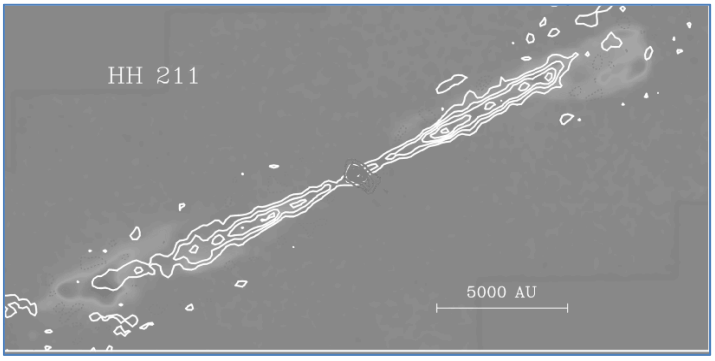

Figure 1.14: Jets and disk in a young stellar object (from IRAM website).

Figure 1.15: Orion Nebula - nearest star formation region (from Hubble gallery).

1.2.4.2 HII Regions: These are regions of ionized hydrogen (HII) usually associated with and present in the giant molecular clouds. Fig 1.15 shows the most extensively observed nearby HII region in Orion (bright regions) created by massive stars. The figure also shows the on-going star formation in nearby regions (darker regions). When massive young stars are formed embedded in a dense molecular cloud, those at the edges of the cloud where the density is not so much as it is in the inner regions, the Extreme-UV radiation flux (Lyman continuum) from the massive protostars ionizes the surrounding matter rich in Hydrogen. The ionization front is impeded at a radial distance R_S from the source (massive young star) when the number of ionizing photons is equal to the number of events of recombination (giving rise to Balmer α line radiation) within the volume defined by the radial distance. Under this assumption Stromgren derived (see e.g., Smith 2004) the size of a HII region for a star of given spectral type as,

$$R_S = 0.032 \left(\frac{N_{UV}}{10^{49}}\right)^{1/3} \left(\frac{n_e}{10^5}\right)^{-2/3} parsec \qquad (1.30)$$

where N_{UV} is the number of UV photons emanating from the star per second (normalised to the numerical factor in the denominator) and n_e is the electron number density normalised to 10^5 per cm^3. Clearly only hot stars of early type can have around them observable sizes of spheres of ionized hydrogen. Therefore, the presence of an HII region is indicative of the

presence of a massive star. Depending upon the angular sizes (based upon the distance of the young star as well as the density of the surrounding matter) the HII regions are divided into categories of normal HII regions (e.g., those in Orion molecular cloud and Trifid nebula); Ultra-Compact HII (UCHII) Regions and Hyper-compact HII (HCHII) regions (see e.g., Churchwell 2002; Zinnecker & York 2007).

As mentioned earlier, massive protostars have K-H timescales much shorter than the free-fall (condensation) timescales (depending only on density) in contrast with the low-mass protostars. For this reason, massive stars attain the zero-age-main sequence phase while still accreting the mass from surrounding parent cloud (see Zinnecker & Yorke 2007). The environment of a massive star can be schematically understood as shown in Fig 1.16. Shown in the figure are layers of regions around a massive star from ionized regions to molecular regions farther from the star where the photon energy decreases below ionizing energy level. The photo-dissociation or photon-dominated regions (PDRs) represent essentially regions where photons having energies around 4.5 eV or larger can dissociate hydrogen molecules (being the most abundant molecule).

During their proto-stellar stages stars of all masses may exhibit features such as jets or outflows and accretion disks. In the case of the low-mass protostars the timescales associated with these manifestations are much longer than for their massive counterparts. For this reason, these features are more widely studied in low-mass stars compared to the massive protostars.

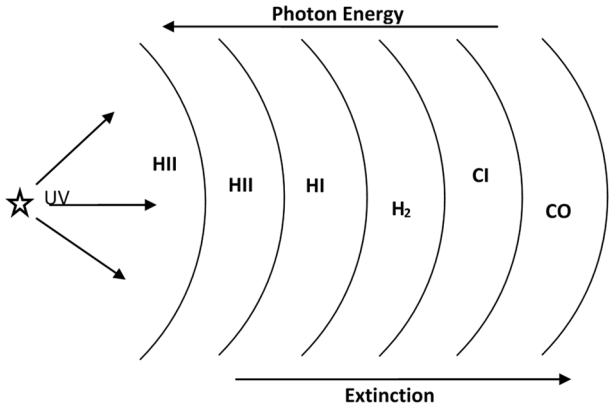

Figure 1.16: Layered structure of a photo-dissociation region (PDR) powered by the UV flux from a massive or hot central star. The energy of photons from near the HII regions (marked HII) towards the edge of neutral atomic region (CI) varies from a few tens of eV to 1 eV. The visual extinction varies from 1 to 10 from the star outwards.

1.2.4.3 Planetary Nebulae: Intermediate stars below about 8 M_0 fail to ignite the nuclear reactions (involving C and O) after the core becomes predominantly made of Carbon and Oxygen. The resulting gravitational collapse is halted only by the electron degeneracy pressure in the core that eventually becomes a White Dwarf. Planetary Nebulae are the result of an episode of heavy mass-loss via a super-wind mechanism following a steady mass-loss during both RGB and AGB stages. The mass loss rates at various stages are:

$$\begin{aligned} \frac{dM}{dt} &= 10^{-9}\, M_{\odot} \quad RGB\ wind\ Mass-loss \\ &= 10^{-7} M_{\odot} \quad AGB\ wind\ Mass-loss \\ &= 10^{-4}\, M_{\odot} \quad Superwind\ mass-loss \end{aligned} \tag{1.31}$$

where $M_{\odot}$ is the solar mass.

The remnant hot core having temperatures more than 50000 K ionizes and excites the surrounding ejected matter. As a result, the tenuous surrounding nebula gives rise to emission in optical and UV region from various atoms of various ionization stages. Some of the most intense line emissions in the visible region come from Hα (Balmer series) at 656.3 nm and doubly ionized oxygen [OIII] at 500.7 nm. More than 60% of the PNe display axially symmetric shapes in the plane of the sky. While it is possible that a large fraction of the galactic intermediate-mass stars could be binaries it is yet to be understood if the tidal force shapes the initial mass-loss during RGB or AGB stage (see Balick & Frank 2002). One of the most intriguing questions is in what way the observed equatorially enhanced density gets formed. The study of the PNe will throw light on the ejection and subsequent shaping mechanisms of the nebular matter and hence the palaeontology of mass loss. Another issue with PNe is to account for the mass that is lost to the ISM – the central object being less than about $1M_{\odot}$ the remaining mass of about a few solar masses needs to be accounted for. The visible nebula accounts for only about a fraction of solar mass; so, it is expected that a large amount of mass is in the form of molecules and possibly dust as well as some portion diffusing away into ISM. Planetary Nebulae enrich the ISM by slow neutron-capture elements by mass loss. For details on planetary nebulae, we may refer to excellent monographs by Pottasch (1983) and Kwok (2000).

In addition to the conventional processes of photoionization and photoexcitation, shock ionization and excitation in ISM also leads to emission from several atoms and their ions.

$$T_s = 1.38 \times 10^5 \left[\frac{v_s}{100} km\, s^{-1}\right]^2 K \qquad (1.32)$$

Here the shock velocity is given by v_s and T_s the temperature attained by the gas in the wake of the shock. While the presence of shock-like projections may be seen in the high-resolution sharp images of several planetary nebulae (see e.g., Fig 1.17), Reipurth & Bally (2001) showed (see Fig 1.18) that several abundant species in the gaseous layers of PNe can be ionized and excited by the shock fronts. High velocities up to 100 km/s are not uncommon in the PNe as several kinematic observations indicate (see e.g., Muthu et al 2001).

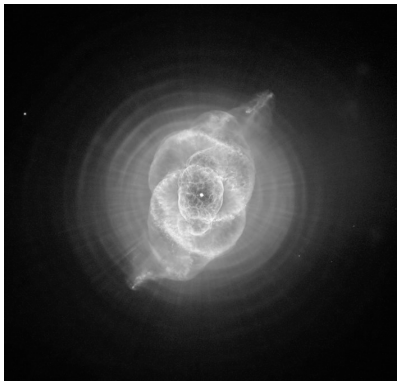

Figure 1.17: Planetary Nebulae - late stages of intermediate stars. The Cat's eye (From Hubble Gallery).

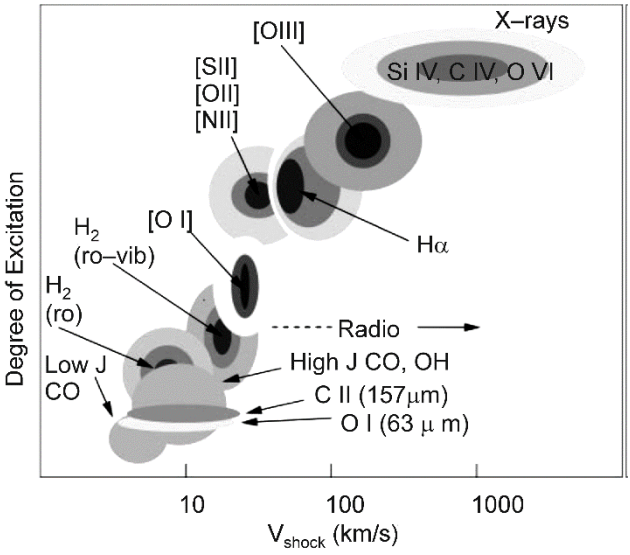

Figure 1.18: Shock Excitation in Nebulae. From Reipurth & Bally 2001.

1.2.4.4 Supernova Remnants: These are the diffuse gaseous matter ejected by a supernova explosion at the end of the journey of evolution of a massive star having mass higher than about 15 $M_\odot$. The gas is rich with heavy elements. Supernova remnants (SNR) are irregular in their morphology

unlike the PNe. Fig 1.19 shows the well-known SNR called the Crab Nebula formed from the Supernova SN 1054 first identified in the year 1054 CE. The diffuse gas may be observed in emission lines from several ionized and neutral species. The energetics of SNR may be derived from observations of such emission lines. Their central objects are either neutron stars (pulsars) or black holes depending upon the initial core mass of their progenitors, required to be more than 3 $M_{\odot}$. SN/SNR enrich the ISM by rapid neutron-capture elements. For details on SN/SNR we may refer to detailed review articles by Weiler & Sramek (1988), Smartt (2009), Janka (2012), Marchant & Bodensteiner (2024).

Figure 1.19: Supernova Remnant - debris from supernova explosion in massive stars - picture shows the famous Crab nebula (from Hubble gallery).

1.2.5 Galaxies: Galaxies such as our Milky Way are large (several kpc in extents) conglomerates of stars and gas (we may refer to the excellent book on the subject by Binney & Tremaine 2008). The number of stars in a galaxy is about a few billions and the total mass that it contains in the form of stars (and gas and dust) is more than 10 billion solar masses. Galaxies are classified into mainly four categories based on their morphology: elliptical (denoted by E) having round shape and smooth distribution of light, spiral (S or SA) having a central bulge and an outer flattened disk, barred spiral (SB) with a central bulge and a bar as well as a flattened disk and irregular galaxies (Irr) having irregular geometrical shape. The elliptical galaxies are further sub-classified depending upon the ratio of their major-to-minor axes (from E0, E1 ….). Similarly, the spirals and barred spirals are sub-classified (into Sa, Sb and so on; and SBa, SBb and so on respectively) by the

"tightness" with which the two spirals are wound. Figure 1.20 shows the classification (known as "Hubble Classification" after the pioneering work of Edwin Hubble) schematically. Fig 1.21 shows the spiral galaxy Messier 81 (M 81) observed by the Hubble Space Telescope (HST).

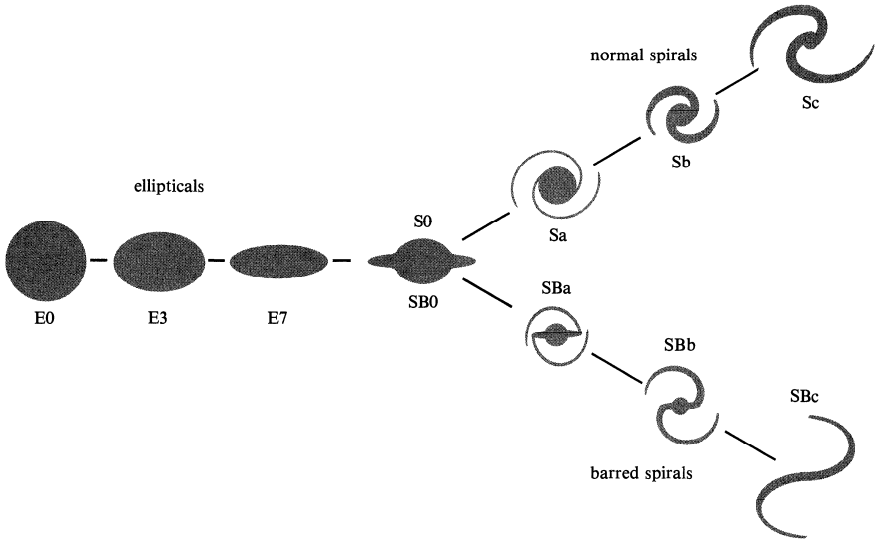

Figure 1.20: Hubble Classification of Galaxies (taken from Shu 1982).

The elliptical galaxies have mostly stellar content with very little gas and dust. Therefore, we usually do not find evidence for recent star formation leading to the presence of young stars in ellipticals. Their component velocities are predominantly random compared to rotational velocities. In spirals the rotational velocities are more predominant. This difference could account for their shapes – roundness in elliptical galaxies and flattened disks in spirals. The elliptical galaxies are also termed as early type while spirals are called late type. Star formation occurs in the spiral arms of both spirals and barred spirals.

The rotational velocities in spirals are expected to be following a rigid body law – increasing with the radial distance from centre – indicating high density of stellar content. Following the bulge however we expect a Keplerian law for rotational velocities - like the planets in Solar System – decreasing with radial distance as $R^{-1/2}$. But the spectroscopic observations of spirals show flattened rotational curves as schematically shown in Fig 1.22. This is indicative of some form of unseen or undetected and yet unknown matter called "dark matter" surrounding the galaxies.

Hubble's law or Hubble-Lemaitre Law: From the redshifts of galaxies Edwin Hubble (Hubble 1929) found out that the receding velocity of a galaxy is

proportional to its distance. This shows that the farther the galaxy is the faster it is receding from the local group. This is called the Hubble's law given by

$$V_G = H_0 \, D_G \tag{1.33}$$

Here V_G and D_G denote the velocity of the galaxy and its distance. H_0 is the proportionality constant famously known as Hubble constant having a value of 50-75 km/s/Mpc. The most inevitable explanation for this path-breaking observational finding is that the Universe is expanding; and hence the Hubble "constant" plays the most crucial role in reconciling with the existing Cosmological theories.

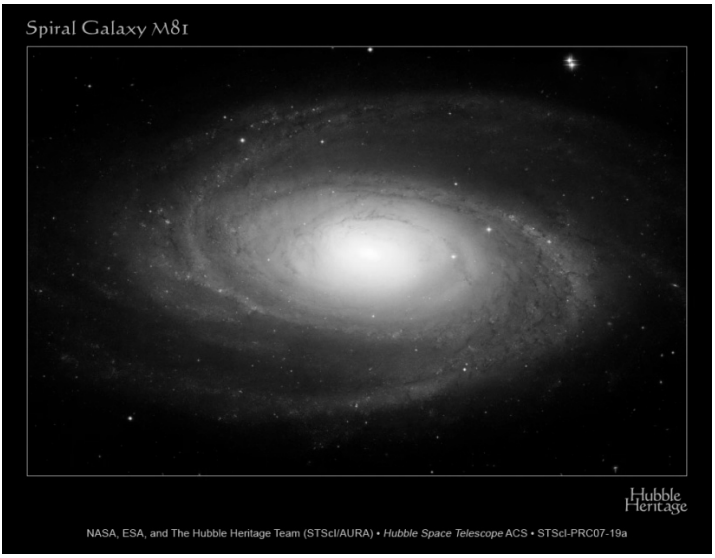

Figure 1.21: The great spiral galaxy M81 (from Hubble gallery).

Apart from the classical elliptical and spiral and irregular galaxies, the extragalactic cosmos presents also an exotic type of sources called Active Galactic Nuclei (AGN) which typically show extraordinarily bright central (nucleus) source putatively embedded in a host galaxy. The central source is thought to be powered by a supermassive Black Hole. Of the AGNs, the Seyfert type of galaxies are relatively nearby as compared to the other types called Quasars and Blazars. For a recent detailed exposition, we may refer to Netzer (2015). A typical spectrum of such sources presenting a bevy of emission lines is shown in Fig 1.23: from Circinus Galaxy (a Seyfert type AGN).

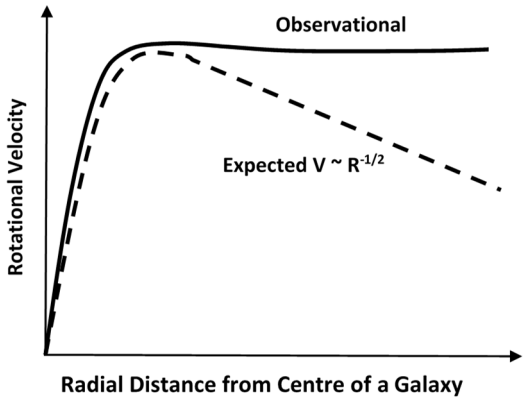

Figure 1.22: Rotational Velocity Curves for Spiral Galaxies showing flatness (from Rubin et al 1985).

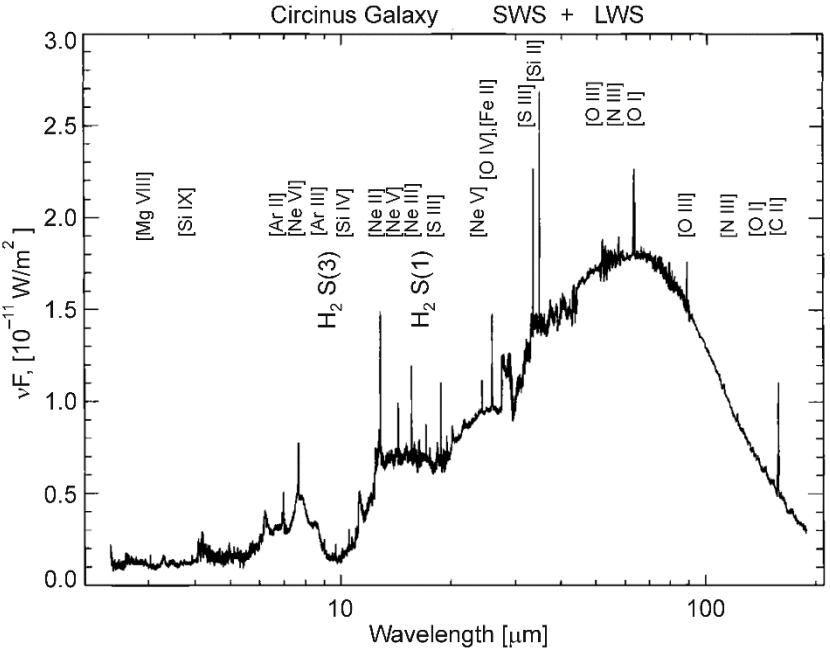

Figure 1.23: ISO infrared spectrum of Circinus Galaxy (from Glass 1999).

1.2.6 Transient Sources: These sources are time-varying on scales of the order of 1 sec and longer. Time resolved and time tagged observations are very important to track the dynamic behaviour of the source. Some well-known examples of such sources are Novae, Supernovae, Outbursts from Young Stellar Objects (YSOs) and Gamma Ray Bursts (GRBs, see e.g., van

Paradijs 2000; Berger 2014). These are objects that display aperiodic or random variability. Objects that vary systematically with highly precise periods such as variable stars and Pulsars do not fall into this category.

1.3 The Forthcoming Chapters

As discussed in the foregoing sections, the celestial sphere offers a variety of sources (called astronomical sources) that are not only very far-off but also very faint in comparative terms, because of their large distances.

We need special instruments to make observations that could unravel the behaviour of these sources. Naked-eye observations, the most ancient and serious pastime for mankind, fascinating even today as it were, had given qualitative account of some of the brightest sources in the sky. However, such unaided observations cannot give deeper (fainter) insight and reliable, non-subjective (objective) and quantitative information. Observations of celestial objects involve measuring the number of photons per unit time, in unit energy (frequency or wavelength) interval and in unit view angle (steradian). These physical quantities are defined in Section 1.1.

Firstly, we need a device, called the telescope, to magnify and collect sufficiently large number of photons. Telescope (usually a parabolic mirror) itself however does not record the photons as they bounce off from its highly reflective surface. We need a suitable optical arrangement to collect the light from the telescope and focus onto a detector to detect and make a record of the detection quantitatively. We discuss these two important tools of observations viz. telescopes and detectors (for visible and near-infrared wavelength regions of electromagnetic spectrum) in Chapter 2 entitled "Telescopes and Detectors".

In Chapter 3 titled "Radiation Processes and Atomic and Molecular Spectroscopy" we discuss the most common or predominant radiation mechanisms in celestial objects which depend on the prevalent physical processes.

Chapter 4 ("Photometric Techniques") discusses astronomical photometry. We discuss instrumentation and techniques used to derive physical parameters concerning celestial objects.

In Chapter 5 titled "Spectroscopic Techniques" we present astronomical spectroscopic instrumentation and techniques to obtain important physical parameters.

Data quality enhancement techniques are discussed in Chapter 6. We conclude in an "Epilogue" by mentioning future directions in Chapter 7.